Effects of molecule-insulator interaction on geometric property of a single phthalocyanine molecule adsorbed on an ultrathin NaCl film

Kuniyuki Miwa,[1] Hiroshi Imada,[1] Shota Kawahara,[1,2] and Yousoo Kim[1,*]
[1]*Surface and Interface Science Laboratory, RIKEN, Wako, Saitama 351-0198, Japan*
[2]*Department of Advanced Materials Science, The University of Tokyo, Kashiwa, Chiba 277-8561, Japan*
(Received 26 February 2016; revised manuscript received 4 April 2016; published 18 April 2016)

The adsorption structure and orientation of a metal-free phthalocyanine (H_2Pc) and a magnesium phthalocyanine (MgPc) on a bilayer of NaCl films were investigated both theoretically and experimentally by means of first-principles calculations based on density functional theory and by scanning tunneling microscopy. H_2Pc is adsorbed with its center over the sodium cation, and H-N bonds in the molecule are aligned with the [100] or [010] surface direction of a bilayer (001)-terminated NaCl film. The most stable structures of MgPc on the NaCl film show two kinds of orientations corresponding to the molecule rotated by $\pm 7^\circ$ relative to the [110] surface direction, with the Mg cation positioned over the chlorine anion in both cases. The energetic barrier for switching between these orientations is as low as 9.0 meV, and during an STM measurement, an orientational change of MgPc can be observed. The interaction between the adsorbed molecule and the NaCl film were analyzed in terms of dispersion interaction, Mg-Cl chemical bonding, and electrostatic interaction. It is found that the small electrostatic interaction between the molecule and the film gives a dominant contribution to determining the molecular orientation. Our detailed and comprehensive studies of the molecule-insulator interaction will provide knowledge to understand and control the properties of molecules on an insulating material.

DOI: 10.1103/PhysRevB.93.165419

I. INTRODUCTION

Geometric and electronic properties of a molecule adsorbed on an insulating material are of great interest in the fundamental science and potential applications for organic (opto)electronic devices such as organic light-emitting diodes (OLEDs) and organic field-effect transistors (OFETs) [1–6]. With recent progress in scanning tunneling microscope (STM) experiments, a few atomic layers of an insulator grown on a conducting substrate provide a novel playground for scientists to investigate molecular properties. Significant features of these films are to partially decouple the molecular electronic structure with the electronic states of the substrate and to still allow electron tunneling into the substrate, enabling the STM measurement of isolated molecules with submolecular spatial resolution [7–14]. Ultrathin films of alkali halide or metal oxide have been introduced to visualize the orbitals of isolated molecules [7–9,15] as well as to improve the efficiency of electroluminescence [16–19] and chemical reaction [20] induced by the tunneling current of STM. In most previous studies, the interaction between the molecule and the ultrathin insulating film was considered small and to have little effect on the properties of molecules. However, the dominant contribution to determining the adsorption structure and orientation of a molecule would be from the molecule-insulator interaction, which can therefore affect the molecular properties related to lateral motion, configuration change, and supramolecular assembly as well as electron transport, electroluminescence, and magnetization phenomena. Thus, there is a need to investigate molecule-insulator interaction in detail in order to understand and control the properties of molecules on an insulating material.

Representatively π-conjugated molecules on ultrathin insulating films have been investigated both theoretically and experimentally [21–28] because these molecules have high thermal and chemical stability and these are important compounds for organic devices [29–33]. Phthalocyanine (Pc) and porphyrin (P), the most common and important π-conjugated molecules, can form a complex with a variety of metal ions, and their electronic, optical, and magnetic properties show robust and exotic characters depending on the metal ion. So far, theoretical and experimental studies on an isolated metal-organic molecule on an insulating film have been done for FePc [34], CuPc and its derivative [35–38], MgP [39], and platinum octaethylporphyrin (PtOEP) [40] on an ultrathin NaCl film as well as Zn etioporphyrin (ZnEtiol) [16], CuPc [41,42], MgP [18,19,43,44], and Zn tetraphenylporphyrin (ZnTPP) [45] on an ultrathin alumina film. To our knowledge, only a few theoretical analyses of these systems from the microscopic viewpoint based on electronic theory have been reported [39,40]. Hence, detailed and comprehensive analyses of the molecule-insulator interaction are in high demand and will provide a novel and essential understanding of their effects on the molecular properties.

In this study, the geometric and electronic properties of a metal-free phthalocyanine (H_2Pc) and a magnesium phthalocyanine (MgPc) adsorbed on ultrathin NaCl films are investigated theoretically and experimentally by means of the first-principles calculations based on density functional theory (DFT) and low-temperature STM. Ultrathin NaCl films are a very promising material because they have a large band gap of 8.9 eV and can be grown as atomically flat layers with various thickness. We chose H_2Pc and MgPc adsorbed on a bilayer NaCl film as a simple model system. The results show that, for H_2Pc on the NaCl film, the center of the molecule is located over the sodium cation (Na top site), and the H-N bond in H_2Pc is in alignment with the [100] or [010] surface direction of a bilayer (001)-terminated

*Corresponding author: ykim@riken.jp

NaCl film. MgPc is adsorbed with the Mg cation over the chlorine anion (Cl top site), and two kinds of orientation are found in which a Mg-N bond is tilted about $\pm 7^\circ$ from the [110] surface direction. The molecule-insulator interaction that determines the adsorption structure and orientation of molecules is analyzed in terms of dispersion interaction, Mg-Cl chemical bonding, and electrostatic interaction.

II. METHODS

First-principles calculations within the framework of DFT were carried out using Vienna Ab initio Simulation Package (VASP) code [46,47]. Ionic cores were described by the projector augmented wave (PAW) method [48,49]. Generalized gradient approximation (GGA) using the Perdew-Burke-Ernzerhof (PBE) functional was utilized to describe the exchange and correlation effects [50]. To take the van der Waals interaction into account, the optB86b version of the non-local van der Waals density functional was adopted [51,52]. Electron density was expanded in a plane-wave basis set with a kinetic-energy cutoff of 480 eV. The electron occupancies are set for each orbital with Gaussian smearing of 0.05 eV. The criterion for total energy convergence is set to 10^{-7} eV, and the structural relaxation calculations were carried out until the minimum force acting on each atom was weaker than 0.01 eV/Å.

The bilayer (001)-terminated NaCl film was modeled by a (6×6) surface unit cell (36 Na cations and 36 Cl anions per layer). The supercell was constructed with a 22-Å vacuum separation between films to reduce the interaction between the films. The lattice constant was set on the basis of the calculated equilibrium lattice constant for the bulk NaCl system of 5.61 Å. To determine the optimized structure of the bilayer NaCl film, we performed preliminary calculations in which all atoms were relaxed. Brillouin-zone integrations were used on a grid of 6×6×1 k points with their origin at the Γ point. The supercell lattice vectors were held fixed during the structural relaxation.

The adsorption of H_2Pc and MgPc on a bilayer of NaCl was considered in all cases, sampling the Brillouin zone with a Γ-centered 1×1×1 k mesh. The adsorption structure and adsorption energies E_{ads} of phthalocyanines on different symmetry sites [as shown in Fig. 1(a)] of the surface of the NaCl films were determined. Here, E_{ads} is defined as

$$E_{ads} = E_{Pc/NaCl} - [E_{Pc} + E_{NaCl}], \quad (1)$$

where $E_{Pc/NaCl}$ is the energy of the whole XPc/NaCl system ($X = H_2$, Mg), E_{Pc} is the energy of a phthalocyanine in the gas phase, and E_{NaCl} is the energy of the clean bilayer NaCl film. Negative values of E_{ads} represent bounded systems, and a smaller value means an energetically stronger molecule-surface binding.

Parts of the figures shown in this paper were visualized using Visualization for Electronic and Structural Analysis (VESTA) software [53].

All experiments were performed with a low-temperature STM (Oxford Instruments) operated at 4.6 K under ultrahigh vacuum (UHV). An STM tip was prepared by electrochemical etching of a silver wire. Ag(111) and Ag(001) substrates are used as metallic substrate underlying NaCl films. The substrate surface was cleaned by repeated cycles of Ar^+ ion sputtering and annealing. NaCl was evaporated using a homemade evaporator heated to 860 K onto the silver substrate at room temperature. H_2Pc and MgPc were used as sample molecules. The molecules were deposited onto the NaCl-covered silver surface at 4.7–12 K cooled in the STM head using another evaporator heated to 675 K for H_2Pc and 750 K for MgPc.

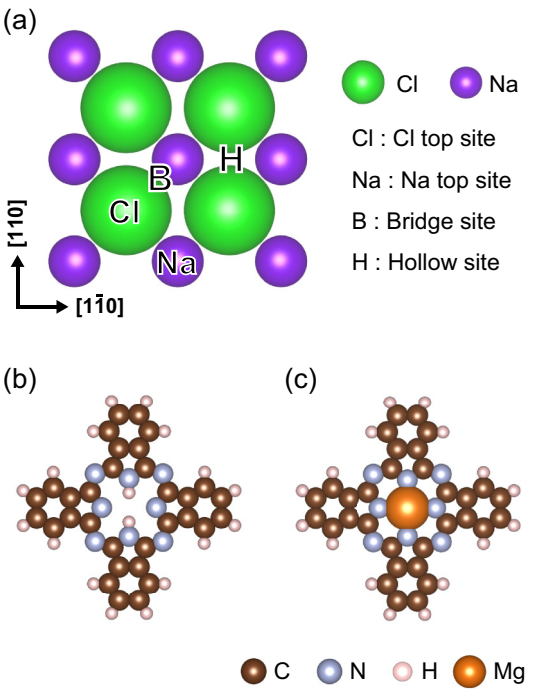

FIG. 1. (a) Top view of the bilayer (001)-terminated NaCl film. The adsorption sites (Cl top, Na top, bridge, and hollow) are indicated. Green and purple spheres show the chlorine and sodium ions, respectively. Molecular structure of (b) metal-free phthalocyanine (H_2Pc) and (c) magnesium phthalocyanine (MgPc). Brown, blue, pink, and orange spheres represent carbon, nitrogen, hydrogen, and magnesium atoms, respectively.

To precisely determine the adsorption structure of molecules, a tip functionalization with a CO molecule was carried out because this significantly increases the spatial resolution of topographic imaging [12,54,55]. For this purpose, CO gas was introduced to the STM head where the crystal is kept at low temperature to codeposit CO molecules with the sample molecules.

III. CALCULATION AND EXPERIMENTAL RESULTS

A. Adsorption site

Adsorption energy E_{ads} for H_2Pc and MgPc on different symmetry sites (Cl top, Na top, bridge, and hollow) is calculated to determine the most stable adsorption site. For a first step to investigate the adsorption geometry, E_{ads} on each site was computed as a function of the molecule-surface distance. Here, the angle ϕ between the [110] surface direction of a bilayer (001)-terminated NaCl film and the H-N bond of H_2Pc (Mg-N bond of MgPc) projected onto the film surface is set to $\phi = 0^\circ$ and 45° so that the system has a high-symmetry structure. Figures 2 and 3 show E_{ads}, which was obtained by single-point calculations with and without including the van

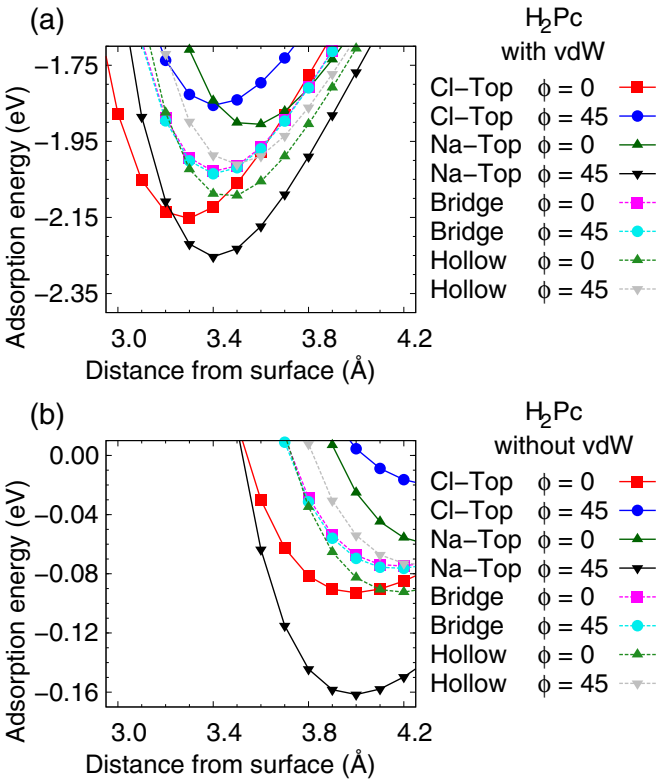

FIG. 2. Adsorption energy E_{ads} for H_2Pc on the bilayer (001)-terminated NaCl film as a function of the distance of H_2Pc from the film surface. The azimuthal angle ϕ between the H-N bond projected onto the film surface and the [110] surface direction is set as $\phi = 0^\circ$ and 45°. The results were obtained by single-point calculations (a) with and (b) without including the van der Waals correction.

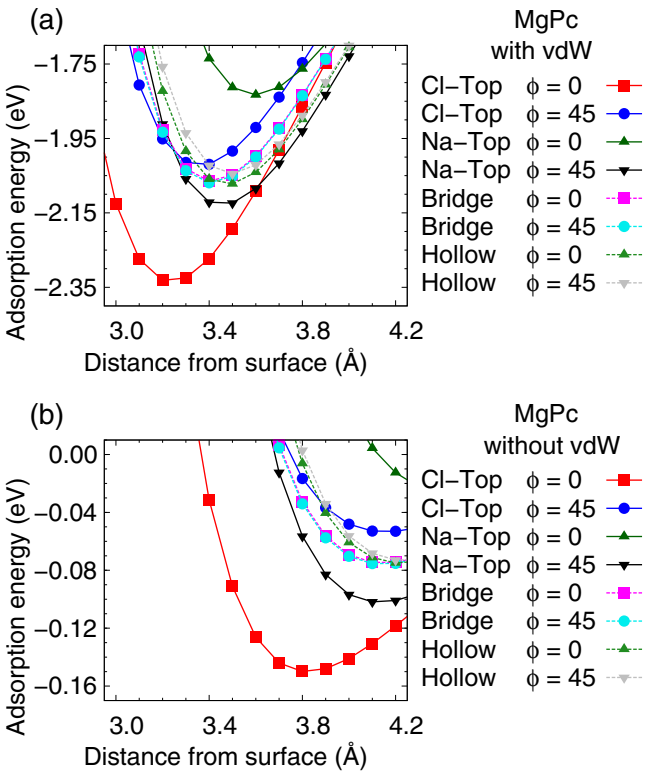

FIG. 3. Adsorption energy E_{ads} for MgPc on the bilayer (001)-terminated NaCl film as a function of the distance of MgPc from the film surface. The azimuthal angle ϕ between the Mg-N bond projected onto the film surface and the [110] surface direction is set as $\phi = 0^\circ$ and 45°. The results were obtained by single-point calculations (a) with and (b) without including the van der Waals correction.

der Waals correction, as a function of the distance between the molecule and the film surface. The energetically stable adsorption site of H_2Pc (MgPc) is on the Na top (Cl top) site with $\phi = 45^\circ$ (with the small ϕ).

The results also show that the dominant contribution to the total adsorption energy is from the van der Waals component. Adsorption energies are vastly different for the cases with and without including the van der Waals correction. Energetically stable distances of molecules from the film surface are also different for two cases.

B. Most stable adsorption structure

The most stable structures of H_2Pc and MgPc were obtained by performing the structural relaxation calculations. The results for H_2Pc are analyzed first, and then those for MgPc are discussed below.

The most stable structure of H_2Pc is shown in Fig. 4(a). The adsorption energy is -2.373 eV, and the H-N bond in H_2Pc is in alignment with the [100] or [010] surface direction. A small distortion in the molecular plane was found upon the adsorption on a bilayer NaCl film. The distance $d_{\text{benzene}-\text{Na}}$ between the benzene rings and the underlying Na^+ cation is about 3.26 Å. The distance $d_{\text{N}-\text{Na}}$ between the aza-bridging N atom and the underlying Na^+ cation is about 3.35 Å.

For the most stable structures of MgPc, two different azimuthal orientations are found corresponding to $\phi = \pm 7^\circ$ with the Mg ion on Cl top sites in both cases [Fig. 4(b)]. The adsorption energy is -2.719 eV, and the distance $d_{\text{Mg}-\text{Cl}}$ between the Mg ion and the underlying Cl^- anion is 2.53 Å.

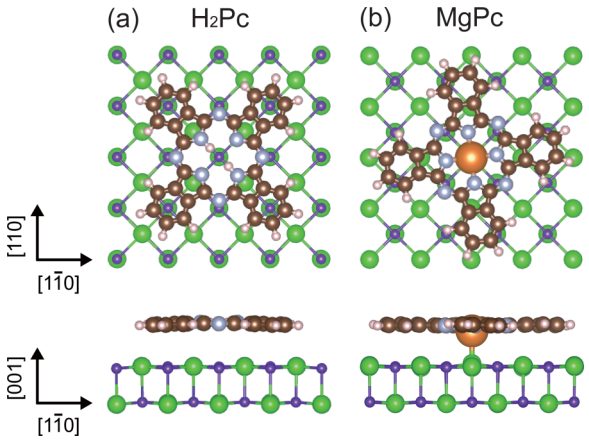

FIG. 4. Top and side views of the most stable structures for (a) H_2Pc and (b) MgPc adsorbed on a bilayer (001)-terminated NaCl film. Green and purple spheres show the chlorine and sodium atoms, respectively. Brown, pink, and blue spheres represent carbon, hydrogen, and nitrogen atoms, respectively. For the MgPc molecule, the central atom is the Mg atom. The angle ϕ between the Mg-N bond projected onto the NaCl surface and the [110] surface direction of bilayer (001)-terminated NaCl film is $+7^\circ$.

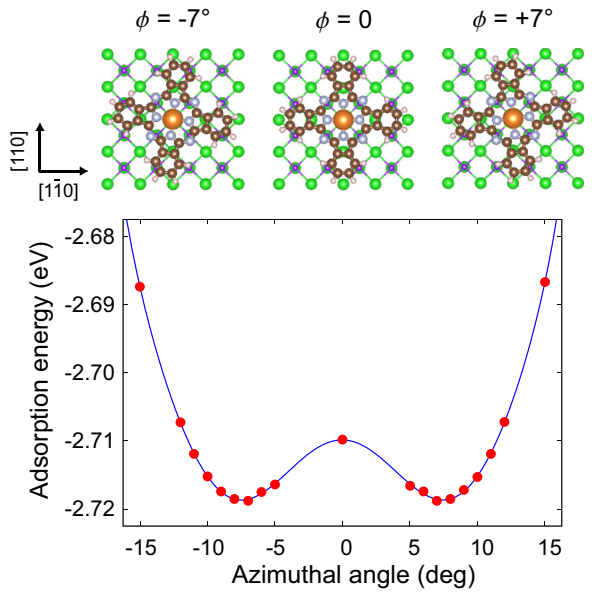

FIG. 5. Adsorption energy E_{ads} for MgPc on the bilayer (001)-terminated NaCl film as a function of the azimuthal angle ϕ between the Mg-N bond projected onto the film surface and the [110] surface direction of the NaCl film. Red dots show the results obtained from DFT calculation. The blue solid line is a polynomial fit.

Here, upon adsorption, the Mg ion is pulled downward by 0.47 Å from the molecular plane, and the Cl^- anion under the Mg ion is pulled up by 0.20 Å. This implies that a chemical bonding between the Mg ion and the Cl^- anion is formed, which is confirmed in the later analysis of the projected density of states (PDOS).

Four benzene rings and four aza-bridging N atoms of MgPc also interact with the substrate. The distance between the benzene ring and the Na^+ cation underneath is about 3.17 Å, and the N-Na distance is about 3.23 Å. The results imply that, in addition to the dispersion force and the Mg-Cl bonding, the small interaction of both benzene rings and aza-bridging N atoms with the NaCl films can affect the adsorption structure and orientation of the molecule.

Figure 5 shows E_{ads} for MgPc adsorbed on the Cl top site of the bilayer NaCl film as a function of the azimuthal angle ϕ. The energetic barrier for the transition between $\phi = \pm 7^\circ$ is 9.0 meV. On the other hand, the energy difference for the cases of $\phi = 7^\circ$ and 45° is much higher, i.e., 285.6 meV. Therefore, MgPc can oscillate between two stable structures with $\phi = \pm 7^\circ$ more easily through the structure with $\phi = 0^\circ$ than through $\phi = 45^\circ$.

C. Experimental results

Our theoretical findings are supported by STM experiments. Figure 6(a) shows the STM topographic image of H_2Pc and MgPc molecules adsorbed on a bilayer NaCl island grown on a Ag(111) substrate. Individual H_2Pc and MgPc molecules are clearly resolved. Their topographic appearance indicates that the aromatic planes of the adsorbed molecules are parallel to the surface and that the azimuthal angles ϕ for H_2Pc and MgPc are different from each other.

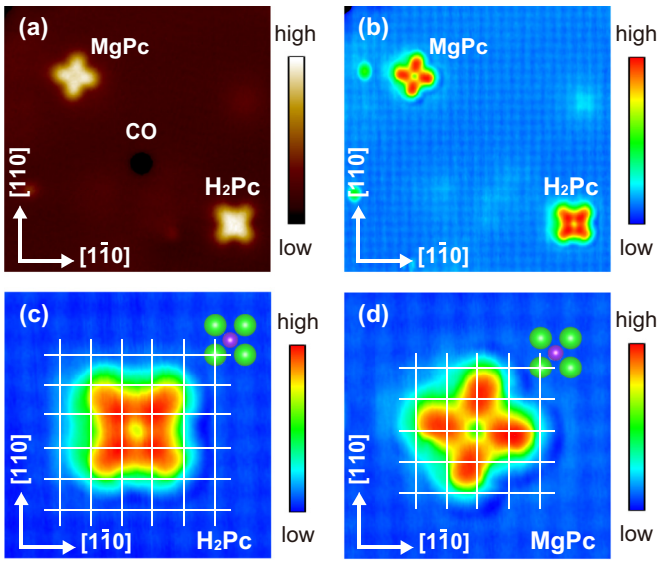

FIG. 6. (a) Constant-current topographic image of H_2Pc and MgPc on a bilayer NaCl island grown on a Ag(111) surface. The image size is 120 by 120 Å. The tunneling gap was set at a sample bias voltage $V_{sample} = -0.550$ V and tunneling current $I_{tunnel} = 5$ pA. CO molecules were codeposited, each of which appears as a dark spot. (b) High-resolution topographic image of the same area as in (a). The image was observed with the STM tip terminated by a CO molecule. The image size is 120 by 120 Å, taken at $V_{sample} = -0.550$ V and $I_{tunnel} = 0.8$ pA. Protrusions correspond to chlorine ions. Green and purple spheres describe the estimated positions of the chlorine and sodium ions, respectively. High-resolution topographic image of (c) H_2Pc and (d) MgPc obtained with the STM tip terminated by a CO molecule. The image size is 40 by 40 Å, taken at $V_{sample} = -0.550$ V and $I_{tunnel} = 1$ pA. Chlorine anions appear as protrusions in a NaCl island. The grid shows the positions of the chlorine anion.

A high-resolution image can be obtained with an STM tip terminated by a CO molecule [12,54,55]. Here, the tip was modified by intentionally picking up a single CO molecule which appears as a dark spot in the STM image [Fig. 6(a)]. Figure 6(b) shows the STM image acquired with a CO functionalized tip. As the positions of the protrusion in a NaCl region are identical in the STM images acquired with a metallic tip and a CO functionalized tip, the protrusions are attributed to Cl anions [55–57]. Figures 6(c) and 6(d) show high-resolution images of H_2Pc and MgPc, respectively. From these results, it is confirmed that the centers of H_2Pc and MgPc are located on the Na and Cl top sites, respectively. For H_2Pc, the direction of a molecular axis is aligned with the [100] and [010] directions of the (001)-terminated NaCl film. MgPc molecules show two kinds of orientation, corresponding to molecules rotated by $\pm 8^\circ (\pm 1^\circ)$ with respect to the [110] surface direction.

All the STM topographic images obtained with a CO functionalized tip show the same adsorption geometry without any exception. In addition, several tens of images were obtained with a metallic tip to confirm that all H_2Pc and MgPc have their unique adsorption geometries. For the sample onto which either H_2Pc or MgPc was deposited, adsorption structure and orientation were similar for the codeposited case.

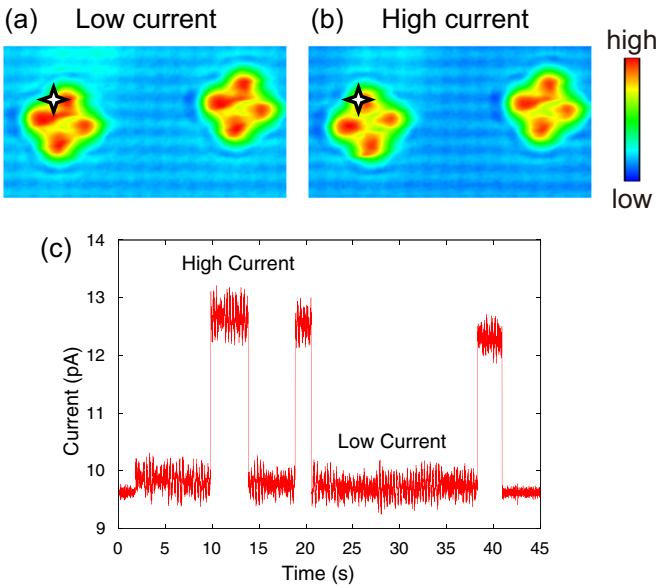

FIG. 7. Constant-current topographic image (a) before and (b) after the configuration change of MgPc. The image was obtained with the STM tip terminated by a CO molecule. The image size is 75×40 Å, taken at $V_{\text{sample}} = -0.550$ V and tunneling current $I_{\text{tunnel}} = 5$ pA. Black stars in the STM images denote the tip position where the current trace is acquired. (c) Tunneling current trace during the configuration change of MgPc observed with the bare STM tip. The tunneling gap was set at a sample bias voltage $V_{\text{sample}} = -0.70$ V.

During the STM observation, MgPc can be reversibly shifted between two stable orientations. The change of molecular orientation is monitored by measuring the tunneling current I as a function of time t while keeping the tip-sample distance constant. Here, the tip is located over the position marked as black stars in Figs. 7(a) and 7(b). In the tunneling current trace shown in Fig. 7(c), the low and high current levels are observed, indicating the switch between two different orientations of MgPc. Figures 7(a) and 7(b) show a sequence of STM images of MgPc molecules in the same area. In Fig. 7(b), MgPc molecules are rotated by about 8° (±1°) relative to the [110] surface direction. The molecules over which the tip is located during the $I - t$ measurement showed an orientational change. Switching between the orientations of MgPc was frequently observed without the lateral translation of the molecular center of mass [39,58,59]. The orientational change of the molecule can also be observed during an STM scan.

The adsorption site and orientation were similar for the molecules adsorbed on a trilayer NaCl film grown on Ag(111) as well as bilayer and trilayer NaCl films grown on Ag(001). The results indicate that the interaction between the molecule and an ultrathin NaCl film gives a dominant contribution to determining the molecular adsorption structures and orientations.

IV. DISCUSSION AND ANALYSIS OF THE ADSORPTION MECHANISM

We analyze the mechanism determining the adsorption characters of phthalocyanine molecules on the basis of further DFT calculations. We investigate the charge density difference

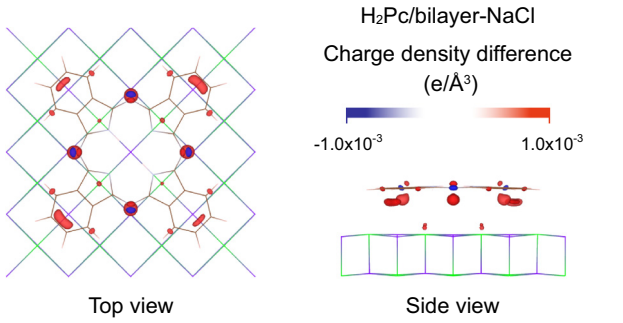

FIG. 8. Charge density difference distribution for H_2Pc adsorbed on the bilayer NaCl film. The value of the isosurface is set to $\pm 0.0010\ e/\text{Å}^3$. Blue and red regions show charge depletion and accumulation, respectively.

$\Delta\rho$, defined as

$$\Delta\rho = \rho_{\text{Pc/NaCl}} - [\rho_{\text{Pc}} + \rho_{\text{NaCl}}], \tag{2}$$

where $\rho_{\text{Pc/NaCl}}$, ρ_{Pc}, and ρ_{NaCl} are the electron densities of the whole XPc/NaCl system ($X = \text{H}_2$, Mg), the isolated phthalocyanine molecule, and the isolated system of the bilayer NaCl film, respectively. Positive and negative values of $\Delta\rho$ indicate, respectively, accumulation and depletion of electron density induced upon the adsorption of a molecule.

Figure 8 shows the spatial distribution of $\Delta\rho$ for H_2Pc on a NaCl film. The accumulation of electron density is found in the regions between the benzene ring and the Na^+ cation as well as the region between the aza-bridging N atom and the underlying Na^+ cation. This suggests the attracting interaction of the benzene rings and the aza-bridging N atom with underlying Na^+ cations. This can be supported by investigating the displacement of the Na^+ cation upon the adsorption of the molecule. The Na^+ cations right under the benzene group are pushed up by 0.11–0.14 Å, and those under the aza-bridging N atoms of MgPc are pushed up by 0.12–0.13 Å. Thus, we conclude that H_2Pc adsorbs on the bilayer NaCl film to minimize both distances $d_{\text{benzene–Na}}$ and $d_{\text{N–Na}}$.

Next, the adsorption character of MgPc is analyzed. We have performed a series of analyses of the PDOS as well as the spatial distribution of the charge density difference $\Delta\rho$ and the electrostatic potential V_{ESP}.

Figure 9 shows the density of states projected on the MgPc, NaCl, and the Mg ion as well as the Cl^- anion right under the Mg ion. A peak appears near −3.54 eV in the PDOS of both the Mg ion and the Cl^- anion [Fig. 9(c)], indicating the hybridization between the Mg p and Cl p orbitals. Further analysis can be carried out by investigating the spatial distribution of $\Delta\rho$. Accumulation of the electron density is observed in the region between the Mg ion and the underlying Cl^- anion (Fig. 10). This rise in electron density represents the formation of the Mg-Cl bond.

Figure 10 also indicates accumulation of the electron density in a region between the benzene group of MgPc and the Na^+ cation of the film. The possible reason is the electrostatic interaction between the π electronic clouds of MgPc with the Na^+ cations. The interaction of π electronic clouds of an aromatic molecule, i.e., benzene, with a single Na^+ cation has been intensively studied over the past few decades [60–64].

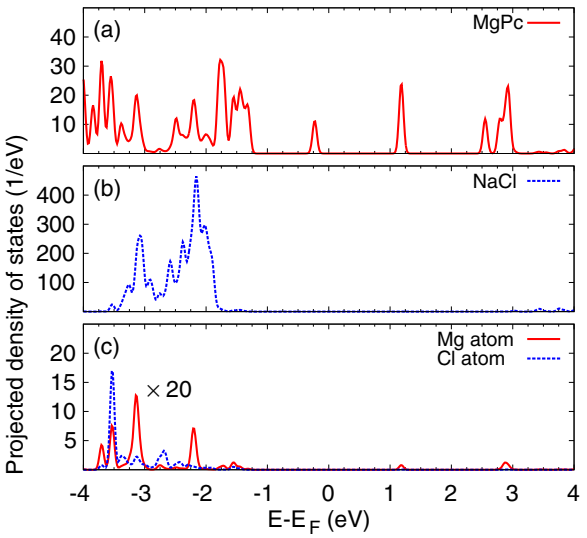

FIG. 9. Density of states projected onto the MgPc, NaCl, the Mg ion, and the Cl ion right under Mg for the MgPc/bilayer-NaCl(001) system.

For the system where a Na^+ cation is positioned perpendicular to the plane of a benzene ring, it has been reported that electrostatic interaction gives a dominant contribution to the cation-π interaction [61,64]. Therefore, to interpret the details of the interaction between MgPc and NaCl, it is essential to investigate the electrostatic potentials.

Figure 11 shows the electrostatic potential V_{ESP} map for an isolated MgPc molecule. As the distance between the molecular plane of MgPc and the NaCl film is about 3.2 Å, we plotted V_{ESP} in a plane at 3.2 Å below the molecular plane. The lowest value of V_{ESP} is observed below the benzene group of MgPc. Here, it should be noted that, in a three-dimensional map of V_{ESP}, the lowest value is found near the aza-bridging N atoms. On the contrary, in a plane 3.2 Å below the molecule, the value of V_{ESP} in a region near the aza-bridging N atoms is higher than that below the benzene group. This result implies that the electrostatic interaction between the benzene group of MgPc and the underlying Na^+ cations plays an important role in determining the molecular orientation.

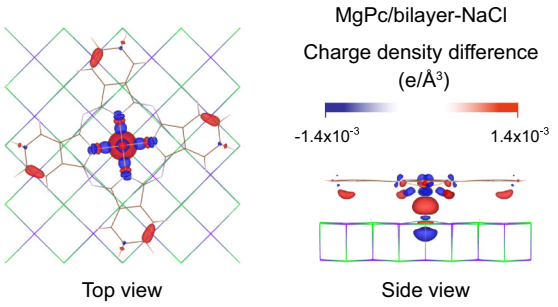

FIG. 10. Charge density difference distribution for MgPc adsorbed on the NaCl film. The value of the isosurface is set to $\pm 0.0014\ e/\text{Å}^3$. Blue and red regions show charge depletion and accumulation, respectively.

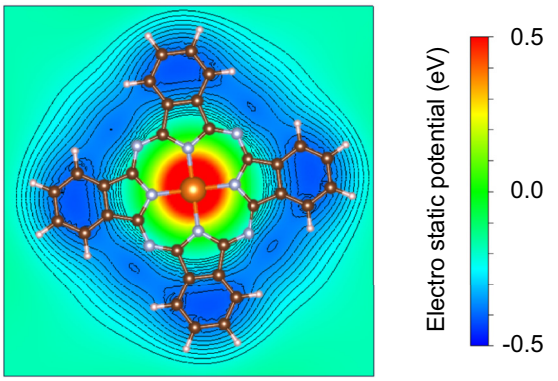

FIG. 11. Spatial distribution of the electrostatic potential for the isolated MgPc molecule plotted in a plane at 3.2 Å below the molecular plane. Red and blue represent electrostatic potential $V_{ESP} = \pm 0.5$ eV, respectively.

This can be supported by analyzing the displacement of the Na^+ cation upon the adsorption of MgPc. The Na^+ cations right under the benzene group are pushed up by 0.12 Å, and those under the aza-bridging N atoms of MgPc are pushed up by 0.06 Å. This result implies that the interaction between the benzene group of MgPc and the underlying Na^+ cations of the NaCl film is stronger than that between the aza-bridging N atom and Na^+. Thus, we concluded that, to minimize the distance between the benzene group and the Na^+ cation, the molecule rotates as shown in Fig. 4(b).

V. CONCLUSIONS

First-principles calculations based on density functional theory were performed to investigate the nature of the adsorption of H_2Pc and MgPc on the bilayer (001)-terminated NaCl film. Dispersion interaction gives a dominant contribution to the adsorption energy. H_2Pc is adsorbed on the Na top site with the distance from the benzene rings and the aza-bridging N atoms to the Na^+ cations minimized. For the adsorption of MgPc, the formation of a chemical bond between the Mg ion and the underlying Cl^- anion makes the Cl top site energetically preferable. Orientation of MgPc is determined to minimize the distance between the benzene rings of the molecule and the Na^+ cations of the NaCl film. It was found that a small electrostatic interaction between the phthalocyanine and the NaCl film plays an essential role in determining the molecular orientation. The adsorption site and configuration of these molecules were confirmed by experimental analysis using a low-temperature scanning tunneling microscope operated under ultrahigh vacuum. High-resolution images obtained with the STM tip terminated by a CO molecule provide powerful evidence for unveiling the adsorption characters.

The present results yield detailed insight into the effects of molecule-insulator interaction on the geometric properties of a π-conjugated molecule adsorbed on an insulating material. Such investigations lead to microscopic understanding of the properties of molecules on an insulating material and therefore will facilitate the design of novel functional materials for organic (opto)electronic devices.

ACKNOWLEDGMENTS

This study was supported in part by JSPS KAKENHI Grants No. 15H02025, No. 26886013, and No. 15J03915. Some of the numerical calculations were performed using RICC and the HOKUSAI system at RIKEN. We thank M. Trenary, R. Arafune, E. Minamitani, and Y. Noda for helpful discussions.

[1] T. Mori, H. Fujikawa, S. Tokito, and Y. Taga, Appl. Phys. Lett. **73**, 2763 (1998).
[2] H. Yanagi and T. Morikawa, Appl. Phys. Lett. **75**, 187 (1999).
[3] C. Dimitrakopoulos and P. Malenfant, Adv. Mater. **14**, 99 (2002).
[4] T. Fukuma, K. Kobayashi, K. Noda, K. Ishida, T. Horiuchi, H. Yamada, and K. Matsushige, Surf. Sci. **516**, 103 (2002).
[5] R. Bennewitz, J. Phys.: Condens. Matter **18**, R417 (2006).
[6] S. A. Burke, J. M. Mativetsky, S. Fostner, and P. Grütter, Phys. Rev. B **76**, 035419 (2007).
[7] J. Repp, G. Meyer, S. M. Stojković, A. Gourdon, and C. Joachim, Phys. Rev. Lett. **94**, 026803 (2005).
[8] J. Repp, G. Meyer, S. Paavilainen, F. E. Olsson, and M. Persson, Science **312**, 1196 (2006).
[9] C. J. Villagomez, T. Zambelli, S. Gauthier, A. Gourdon, C. Barthes, S. Stojkovic, and C. Joachim, Chem. Phys. Lett. **450**, 107 (2007).
[10] P. Liljeroth, J. Repp, and G. Meyer, Science **317**, 1203 (2007).
[11] A. Safiei, J. Henzl, and K. Morgenstern, Phys. Rev. Lett. **104**, 216102 (2010).
[12] L. Gross, Nat. Chem. **3**, 273 (2011).
[13] T. Leoni, O. Guillermet, H. Walch, V. Langlais, A. Scheuermann, J. Bonvoisin, and S. Gauthier, Phys. Rev. Lett. **106**, 216103 (2011).
[14] J. Henzl, P. Puschnig, C. Ambrosch-Draxl, A. Schaate, B. Ufer, P. Behrens, and K. Morgenstern, Phys. Rev. B **85**, 035410 (2012).
[15] J. Guo, X. Meng, J. Chen, J. Peng, J. Sheng, X.-z. Li, L. Xu, J.-r. Shi, E. Wang, and Y. Jiang, Nat. Mater. **13**, 184 (2014).
[16] X. H. Qiu, G. V. Nazin, and W. Ho, Science **299**, 542 (2003).
[17] E. Ćavar, M. C. Blüm, M. Pivetta, F. Patthey, M. Chergui, and W. D. Schneider, Phys. Rev. Lett. **95**, 196102 (2005).
[18] S. W. Wu, G. V. Nazin, and W. Ho, Phys. Rev. B **77**, 205430 (2008).
[19] C. Chen, P. Chu, C. A. Bobisch, D. L. Mills, and W. Ho, Phys. Rev. Lett. **105**, 217402 (2010).
[20] H.-J. Shin, J. Jung, K. Motobayashi, S. Yanagisawa, Y. Morikawa, Y. Kim, and M. Kawai, Nat. Mater. **9**, 442 (2010).
[21] J. Repp and G. Meyer, Appl. Phys. A **85**, 399 (2006).
[22] L. Gross, F. Mohn, N. Moll, P. Liljeroth, and G. Meyer, Science **325**, 1110 (2009).
[23] F. Mohn, J. Repp, L. Gross, G. Meyer, M. S. Dyer, and M. Persson, Phys. Rev. Lett. **105**, 266102 (2010).
[24] L. Gross, N. Moll, F. Mohn, A. Curioni, G. Meyer, F. Hanke, and M. Persson, Phys. Rev. Lett. **107**, 086101 (2011).
[25] F. Mohn, L. Gross, N. Moll, and G. Meyer, Nat. Nanotechnol. **7**, 227 (2012).
[26] K. Morgenstern, N. Lorente, and K.-H. Rieder, Phys. Status Solidi B **250**, 1671 (2013).
[27] N. Pavliček, I. Swart, J. Niedenführ, G. Meyer, and J. Repp, Phys. Rev. Lett. **110**, 136101 (2013).
[28] F. Albrecht, M. Neu, C. Quest, I. Swart, and J. Repp, J. Am. Chem. Soc. **135**, 9200 (2013).
[29] J. H. Burroughes, D. D. C. Bradley, A. R. Brown, R. N. Marks, K. Mackay, R. H. Friend, P. L. Burns, and A. B. Holmes, Nature (London) **347**, 539 (1990).
[30] F. Garnier, R. Hajlaoui, A. Yassar, and P. Srivastava, Science **265**, 1684 (1994).
[31] K. Yamada, T. Okamoto, K. Kudoh, A. Wakamiya, S. Yamaguchi, and J. Takeya, Appl. Phys. Lett. **90**, 072102 (2007).
[32] S. Maier, L.-A. Fendt, L. Zimmerli, T. Glatzel, O. Pfeiffer, F. Diederich, and E. Meyer, Small **4**, 1115 (2008).
[33] M. Kittelmann, P. Rahe, M. Nimmrich, C. M. Hauke, A. Gourdon, and A. Kühnle, ACS Nano **5**, 8420 (2011).
[34] A. Scarfato, S.-H. Chang, S. Kuck, J. Brede, G. Hoffmann, and R. Wiesendanger, Surf. Sci. **602**, 677 (2008).
[35] T. Sonnleitner, I. Swart, N. Pavliček, A. Pöllmann, and J. Repp, Phys. Rev. Lett. **107**, 186103 (2011).
[36] I. Swart, T. Sonnleitner, and J. Repp, Nano Lett. **11**, 1580 (2011).
[37] I. Swart, T. Sonnleitner, J. Niedenführ, and J. Repp, Nano Lett. **12**, 1070 (2012).
[38] C. Uhlmann, I. Swart, and J. Repp, Nano Lett. **13**, 777 (2013).
[39] S. Yan, Z. Ding, N. Xie, H. Gong, Q. Sun, Y. Guo, X. Shan, S. Meng, and X. Lu, ACS Nano **6**, 4132 (2012).
[40] S. H. Kim, H. Jeong, S. Lim, U. Ham, Y. Song, J. Yu, and Y. Kuk, Surf. Sci. **613**, 54 (2013).
[41] S. W. Wu, G. V. Nazin, X. Chen, X. H. Qiu, and W. Ho, Phys. Rev. Lett. **93**, 236802 (2004).
[42] X. H. Qiu, G. V. Nazin, and W. Ho, Phys. Rev. Lett. **92**, 206102 (2004).
[43] S. W. Wu, N. Ogawa, and W. Ho, Science **312**, 1362 (2006).
[44] S. W. Wu, N. Ogawa, G. V. Nazin, and W. Ho, J. Phys. Chem. C **112**, 5241 (2008).
[45] Y. Zhang, F. Geng, H. Y. Gao, Y. Liao, Z. C. Dong, and J. G. Hou, Appl. Phys. Lett. **97**, 243101 (2010).
[46] G. Kresse and J. Furthmüller, Phys. Rev. B **54**, 11169 (1996).
[47] G. Kresse and J. Furthmüller, Comput. Mater. Sci. **6**, 15 (1996).
[48] P. E. Blöchl, Phys. Rev. B **50**, 17953 (1994).
[49] G. Kresse and D. Joubert, Phys. Rev. B **59**, 1758 (1999).
[50] J. P. Perdew, K. Burke, and M. Ernzerhof, Phys. Rev. Lett. **77**, 3865 (1996).
[51] J. Klimeš, D. R. Bowler, and A. Michaelides, J. Phys.: Condens. Matter **22**, 022201 (2010).
[52] J. Klimeš, D. R. Bowler, and A. Michaelides, Phys. Rev. B **83**, 195131 (2011).
[53] K. Momma and F. Izumi, J. Appl. Crystallogr. **44**, 1272 (2011).
[54] L. Bartels, G. Meyer, and K.-H. Rieder, Appl. Phys. Lett. **71**, 213 (1997).
[55] L. Gross, F. Mohn, N. Moll, G. Meyer, R. Ebel, W. M. Abdel-Mageed, and M. Jaspars, Nat. Chem. **2**, 821 (2010).
[56] W. Hebenstreit, J. Redinger, Z. Horozova, M. Schmid, R. Podloucky, and P. Varga, Surf. Sci. **424**, L321 (1999).

[57] J. Repp, S. Fölsch, G. Meyer, and K.-H. Rieder, Phys. Rev. Lett. **86**, 252 (2001).
[58] J. Schaffert, M. C. Cottin, A. Sonntag, H. Karacuban, C. A. Bobisch, N. Lorente, J.-P. Gauyacq, and R. Möller, Nat. Mater. **12**, 223 (2013).
[59] G. Antczak, W. Kamiński, A. Sabik, C. Zaum, and K. Morgenstern, J. Am. Chem. Soc. **137**, 14920 (2015).
[60] J. C. Ma and D. A. Dougherty, Chem. Rev. **97**, 1303 (1997).
[61] E. Cubero, F. J. Luque, and M. Orozco, Proc. Natl. Acad. Sci. USA **95**, 5976 (1998).
[62] C. Garau, A. Frontera, D. Quiñonero, P. Ballester, A. Costa, and P. M. Deyà, Chem. Phys. Lett. **399**, 220 (2004).
[63] C. Garau, A. Frontera, D. Quiñonero, P. Ballester, A. Costa, and P. M. Deyà, Chem. Phys. Lett. **392**, 85 (2004).
[64] S. E. Wheeler and K. N. Houk, J. Am. Chem. Soc. **131**, 3126 (2009).